Am J Cardiovasc Dis 2013;3(1):1-16
www.AJCD.us /ISSN:2160-200X/AJCD1211003

Review Article

Bifurcation theory and cardiac arrhythmias

Hrayr S Karagueuzian, Hayk Stepanyan, William J Mandel

From the Translational Arrhythmia Research Section, UCLA Cardiovascular Research Laboratory and the Division of Cardiology, Departments of Medicine David Geffen School of Medicine at UCLA, Los Angeles, California

Received November 26, 2012; Accepted January 16, 2013; Epub February 17, 2013; Published February 27, 2013

Abstract: In this paper we review two types of dynamic behaviors defined by the bifurcation theory that are found to be particularly useful in describing two forms of cardiac electrical instabilities that are of considerable importance in cardiac arrhythmogenesis. The first is action potential duration (APD) alternans with an underlying dynamics consistent with the period doubling bifurcation theory. This form of electrical instability could lead to spatially discordant APD alternans leading to wavebreak and reentrant form of tachyarrhythmias. Factors that modulate the APD alternans are discussed. The second form of bifurcation of importance to cardiac arrhythmogenesis is the Hopf-homoclinic bifurcation that adequately describes the dynamics of the onset of early afterdepolarization (EAD)-mediated triggered activity (Hopf) that may cause ventricular tachycardia and ventricular fibrillation (VT/VF respectively). The self-termination of the triggered activity is compatible with the homoclinic bifurcation. Ionic and intracellular calcium dynamics underlying these dynamics are discussed using available experimental and simulation data. The dynamic analysis provides novel insights into the mechanisms of VT/VF, a major cause of sudden cardiac death in the US.

Keywords: Period-doubling bifurcation, Hopf-homoclinic bifurcation, action potential duration alternans, early afterdepolarization, triggered activity, spatially-discordant alternans, reentry, ventricular tachycardia, ventricular fibrillation

Bifurcation theory is the mathematical study of changes in the qualitative behavior of diverse nonlinear dynamical systems including the electrical activity of cardiac myocyte [1, 2]. A nonlinear system, unlike a linear one, is a system whose output is not proportional to the input, and bifurcation is said to occur when a small change made to the system's parameter value(s) causes a dramatic qualitative changes in appearance. Cardiac myocytes are perfect examples of nonlinear systems with their nonlinear voltage current profiles and with their characteristic property to manifest sudden transitions to a different cardiac rhythm [3]. The changes in nonlinear systems are sudden and unexpected (bifurcations) that linear reasoning fails to explain the newly emerged dynamics. The term "bifurcation" was coined by Henri Poincaré in 1885 based on his observations on the nonlinear dynamic behavior of fluids subjected to stressful perturbations [4]. The application of the bifurcation theory in cardiac electrophysiology provided mechanistic insights into the nature of irregular beat-to-beat electrical activity (instability) [5-7] and paved the way to conceptually novel and effective therapeutic approaches designed to prevent arrhythmogenic cellular electrical instability [8] that linear approaches could not achieve. The bifurcation theory is found to be particularly useful in describing two forms of cardiac electrical instabilities that are of considerable importance in cardiac arrhythmogenesis and which will be the focus of this review. The first is electrical alternans with an underlying dynamics consistent with the period doubling bifurcation theory that also explains the emergence of beat-to-beat irregular cellular action potential properties (i.e., chaos) that emerge in stresses cardiac myocytes [5, 9-12]. The second arrhythmogenic mechanism is the onset of early afterdepolarization (EAD)-mediated triggered activity, a dynamic scenario that is adequately explained by the Hopf bifurcation theory. Furthermore, the patterns by which the EAD-mediated triggered activity often terminates can also be adequately explained by yet another bifurcation theory, the homoclinic bifurcation

making the Hopf-homoclinic dual bifurcation theory to fully account for the experimentally observed initiation and self-termination of EAD-mediated triggered activity in cardiac tissue. While the theory does not provide insight into individual ionic current mechanisms by which a sudden electrical instability emerges, it however provides two important insights. First, it defines the general necessary parametric changes (i.e., kinetics of inward vs. kinetics of outward currents) that are necessary for a specific electrical instability to emerge, and second it permits making predictions of an impending instability based on key electrical parameter(s) of the cardiomyocyte. Complimentary simulation studies using realistic cardiac cell models are needed to unravel the specific individual ionic current(s) kinetics responsible for the observed dynamical instability (bifurcation) [8, 13-15].

In the first part of this review we will discuss how cardiac cellular instability caused by the period doubling bifurcation scenario leads to temporal beat-to-beat action potential duration (APD) alternans of cardiac myocytes and then discuss the factors at the whole heart level that modulate the transition from spatially concordant form of APD alternans, during which APD is either short or long everywhere in the ventricles to spatially discordant form of APD alternans (SDA), where short APD coexists with long APD of the same ventricle separated by nodal lines where APD does not change. **Figure 2** illustrates schematically the phenomenon of SDA alternans and **Figure 4** shows a transition from spatially concordant to SDA alternans leading to VF in an isolated aged rate heart subjected to stress. The SDA (unlike concordant) leads to reentrant form ventricular tachycardia (VT) [16-21], and is classically described in the literature as VT caused by "dispersion of repolarization" [22-24]. In the second part of this review we discuss EAD-mediated triggered activity (Hopf bifurcation) and its subsequent self-termination (homoclinic bifurcation). The triggered activity causes a focal form of VT during which successive beats arise from a well-circumscribed site [14, 20, 21, 25-27]. The rate of the VT caused by focal mechanism is fast enough to promote SDA causing a transition from a focal or a single reentrant VT to ventricular fibrillation (VF), a major cause of sudden cardiac death in the US [28]. We need to mention here that while these dynamic scenarios are also applicable to atrial arrhythmias [29-31], we however, in this review will focus only on VT/VF.

Period doubling bifurcation & the emergence of spatially discordant APD alternans

It was in 1910 when Sir Thomas Lewis made the following remarkable observation in his experimental studies:

"Heart alternation occurs under two circumstances. It is seen when the cardiac muscle is not of necessity altered structurally, as an accompaniment of great acceleration of the rate of rhythm. It is also found when the pulse is of normal rate, and under such circumstances the muscle is either markedly degenerate or the heart shows evidence of embarrassment as a result of poisoning or some other factor" [32].

Importantly, Lewis further emphasized that such electrical anomaly observed in experimental studies was also observed in humans:

"The electrocardiographic curves obtained in clinical heart alternation are similar to those obtained experimentally; there is divergence between the heights of R and T and the amplitude of the radial upstrokes. These facts demonstrate the identity of the clinical and experimental conditions" [32].

While cardiac electrical alternans was known to emerge in diseased hearts in experimental and clinical settings, it was only during the last two decades that the importance of cellular APD alternans in the genesis of reentrant arrhythmias was elucidated in animal models [17, 20], and its role in the form of electrocardiographic T wave alternans in increasing the risk of sudden cardiac death in man was recognized [33, 34].

The mechanism of cardiac electrical alternans was extensively studied in animal models that scaled from in situ and isolated-perfused hearts to isolated bits of perfused cardiac tissues down to isolated single cardiac myocytes using the patch-clamp technique. The introduction of the optical mapping technique using voltage-sensitive fluorescent dye allowed the determination of cardiac depolarization and

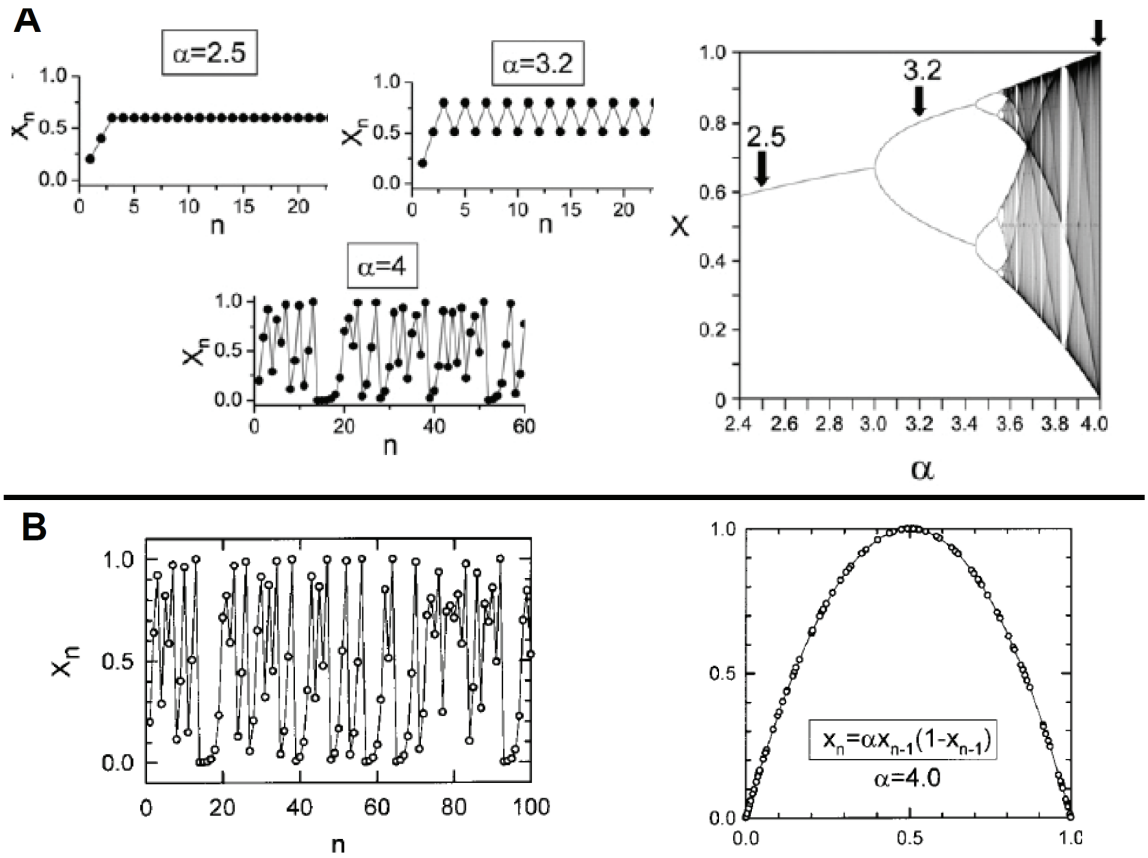

Figure 1. *Dynamical chaos in the logistic equation*. A: iteration of the logistic equation as a function of increasing values of α producing different behaviors, starting with periodic (α=2.5), alternating (α=3.2) and completely irregular (chaotic) behavior with α=4 respectively. The curve on the right of panel A side is bifurcation diagram showing steady-state behavior as a function of α. In panel B (left) shows sequential data set (Xn) with very irregular beat-to-beat pattern (chaos) pattern. A plot of this set of data (panel B right) in which the current value of X is plotted against its previous value, shows nonlinear relationship described by the logistic equation (inset). The height of the parabola is defined by the slope of ascending limb of the parabola α, i.e., the dynamic equivalent of the slope of the APD restitution curve (*From Weiss et al*. [99]).

repolarization over large surfaces of cardiac tissue with high tempo-spatial resolution. Additionally direct examination of the underlying intracellular Ca ion (Ca_i^{2+}) dynamics using Ca-sensitive fluorescent dye provided important insight into the role of Ca_i^{2+} dynamics in the genesis and modulation of the cellular APD alternans. The combined isolated myocytes and whole heart studies provided insight into the mechanism of APD alternans at the single cell level and defined the factors that promote the transition from spatially concordant to SDA in the whole heart. We now discuss the factors that influence cellular vulnerability to APD alternans that promote the emergence of spatially discordant APD alternans in the whole heart leading to VT/VF.

Alternans and the slope of the APD restitution curve

The slope of the APD restitution was classically used as a major marker of APD alternans when Nolasco & Dhal in 1968 first mathematically analyzed the curve constructed by plotting the APD vs. its diastolic interval [35]. The curve thus obtained, the APD restitution curve, represents the gain in APD as the diastolic interval is lengthened is also demonstrated to occur in human hearts using monophasic APs and is popularly known as “electrical restitution” [36]. In strict mathematical terms it is shown that when the slope of the APD restitution curve is >1, then slight perturbation in the rate or rhythm of the heart will promote APD alternans

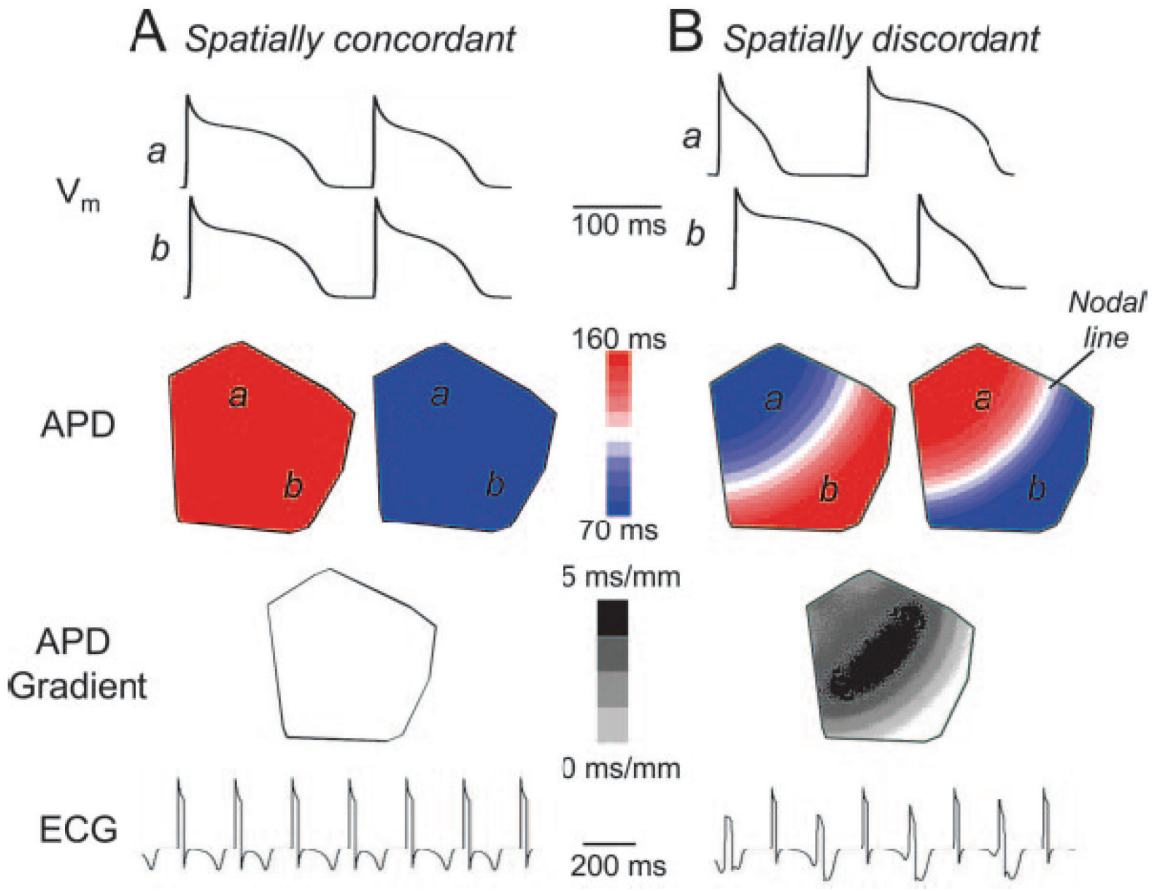

Figure 2. *Schematic illustrations of simulated 2D spatially concordant and discordant APD alternans.* A: Top traces show that simulated action potentials from sites *a* and *b* both alternate in a long-short pattern during pacing at 220-ms CL. Second panel shows that the spatial APD distribution is either long (red) or short (blue) for each beat. Third panel shows that the APD dispersion (gray scale) for either long or short beats is minimal. Bottom panel shows simulated electrocardiogram (ECG), with T wave alternans. Panel B, top traces show that at a pacing CL of 180 ms, simulated action potentials from site *a* now alternate short-long, whereas at the same time, action potentials from site *b* alternate long–short. Second panel shows the spatial APD distribution, with a nodal line (white) with no APD alternation separating the out-of-phase top and bottom regions. Third panel shows that the APD dispersion is markedly enhanced, with the steepest gradient (black) located at the nodal line. Bottom panel shows simulated ECG, with both T wave and QRS alternans (attributable to engagement of CV restitution), as observed experimentally (*From Weiss et al*. [42]).

and irregular beat to beat AP dynamics (chaos) in aggregates of chick myocytes [6, 37] and in stressed isolated mammalian cardiac tissue [9-12, 38]. **Figure 1** illustrates APD dynamics. In contrast however, when such perturbations are applied in hearts with APD restitution slope <1 no alternans or irregular dynamics emerge [35]. More recently, taking advantage of interventions designed to control chaotic dynamics, Garfinkel and associates successfully applied chaos control algorithm (i.e., critically timed pacing protocol) to regularize irregular (chaotic) beat-to-beat AP dynamics in isolated perfused rabbit ventricular tissue intoxicated with ouabain [39]. As suggested by Lewis more than a century ago, we showed that ventricular tissue isolated from arrhythmic ventricle intoxicated with quinidine overdose indeed manifests APD alternans and irregular (chaotic) dynamics at pacing rates that normal tissue do not manifest either APD alternans or irregular (chaotic) dynamics [12]. **Figure 1** schematically shows the period doubling bifurcation diagram and demonstrates how a parameter change in a simple equation called the logistic equation, causes the emergence of not only APD alternans but also beat-to-beat irregular (chaotic) APD dynamics. The equation describes the evo-

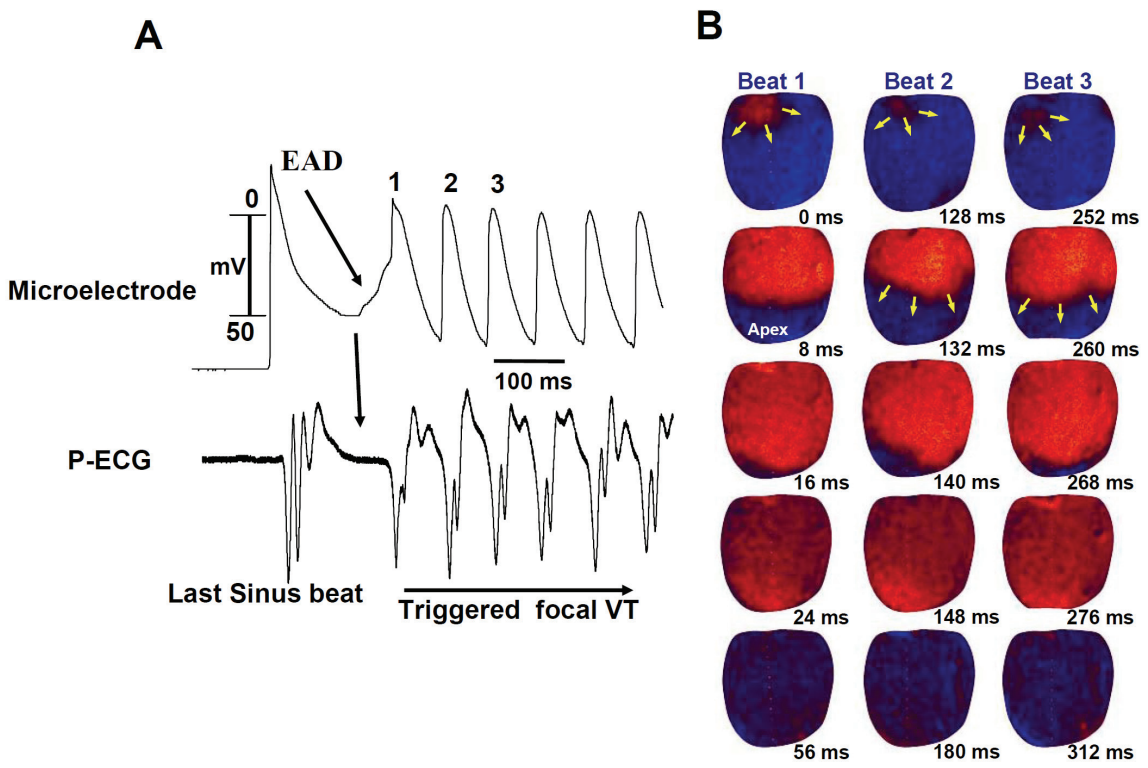

Figure 3. *EAD-mediated triggered activity causing focal ventricular tachycardia.* Panel A shows simultaneous microelectrode and ECG recording from an isolated aged rat heart subjected to oxidative stress with hydrogen peroxide. EAD-mediated triggered activity (arrow) arises as a focal activity from the base of the heart as shown during simultaneous optical mapping (snap shots in panel B) using voltage-sensitive dye. The depolarizing wavefront (red) propagates as a single wavefront toward the apex. In each snap shot activation time in ms is shown at the bottom right with time zero (arbitrary) coinciding with the onset of beat #1. Activation map of the first three beats (#1, #2, & #3) are shown which correspond to the three beats (1, 2 & 3) shown with the microelectrode recording. Notice that the mergence of the EAD coincides in time with the isoelectric interval on ECG (downward vertical arrow) indicating that no other activity precedes the when EAD-mediated triggered focal activity emerges near the base of the heart. Yellow arrows in panel B indicate the direction of wavefront propagation *(Previously unpublished)*.

lution of successive changes of the APD (x_n, x_{n+1},...) as a function of the slope of APD restitution curve, equivalent to the parameter α in the logistic equation:

$x_{n+1} = \alpha . x_n (1-x_n)$ (**Figure 1**) If we assign an initial value to x_0 (between 0 and 1) then use the logistic equation the next value x_1 from x_0, then x_2 from x_1, and so forth the qualitative outcome depends strongly on the value of α (i.e., the slope of APD restitution curve) showing alternans and irregular (chaos) APDs as shown in **Figure 1**.

Alternans and intracellular Ca (Ca_i^{2+}) dynamics

While the slope of the APD restitution curve could modulate and even control APD alternans under certain conditions [31], more recent studies convincingly demonstrated that the diastolic interval (DI) alone was an insufficient marker to fully explain the phenomenon of APD alternans. The highly interactive intra- and transmembrane cellular events that take place during the course of an AP contribute importantly to the phenomenon of APD alternans. Perhaps one of the most important factor is the intracellular Ca (Cai) cycling dynamics that plays a key role in the genesis of APD alternans [40-43]. Using simultaneous voltage and Cai fluorescent dyes it is shown both in tissue [40] and isolated ventricular myocytes [41], that the APD alternans becomes invariably prevented by the suppression of the sarcoplasmic reticulum (SR) Cai cycling, and that APD alternans occurs irrespective of the steepness of the slope of APD restitution curve [41]. Moreover, it is found in intact ventricle that the endocardium, despite having a flatter APD restitution

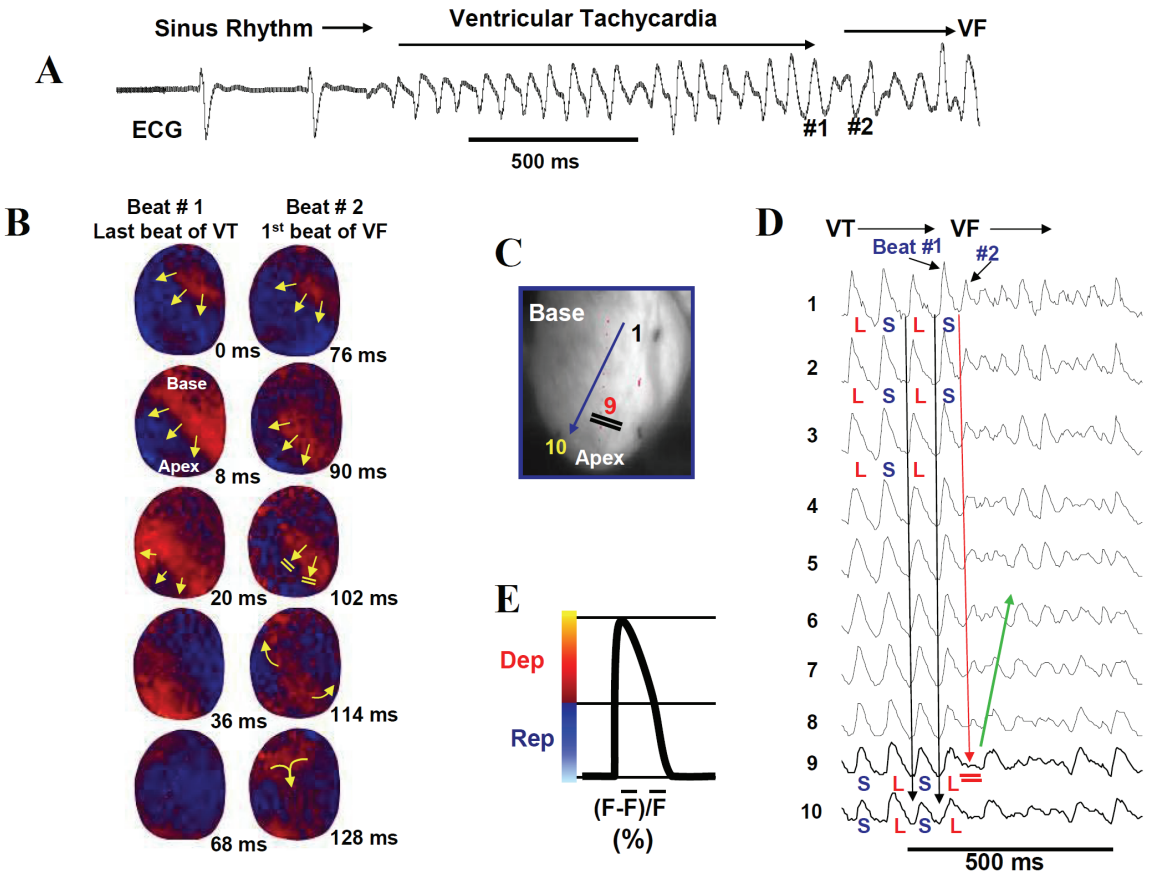

Figure 4. *Initiation of focal VT & transition to VF caused by the emergence of spatially discordant.* Panel A is a pseudo-ECG in isolated-perfused aged rat heart exposes to glycolytic inhibition that promotes EADs and triggered activity. The ECG shows the last 2 sinus beats before the sudden onset of the VT that leads to VF. Panel B, shows snap shots of the first and the last beat of the VT followed by the first beat of the VF. The VT is caused by a focal activation arising from the base of the heart that propagates without block (yellow arrows; snap shots, 0 to 68 ms). However, the beat after the last VT beat undergoes functional conduction block toward the apex (snap shots, 102) and shown schematically by double horizontal lines in *C*. The front, however continues to propagate laterally on both sides of the block, causing Figure- 8 reentry and subsequent transition from VT to VF as shown in the ECG. Panel shows optical action potentials recorded from base to apex (numbered 1 to 10) during the last 4 VT beats and at the onset of VF showing that the site of block corresponds to the site of long APD (double horizontal red lines) during the emergence of spatially discordant APD alternans. After the conduction block the direction of the propagation changes (green arrow) signaling the onset of a reentrant activation. In each snap shot the activation time is in milliseconds (bottom right) with time zero (arbitrary) coinciding with the onset of beat 1 and subsequent VT beats. The red color in the snap shots represents depolarization (Dep) and the blue repolarization (Rep) as shown in E. Downward pointing arrows indicate the direction of propagation. L, long; S, short (From Morita et al. [21]).

slope than the epicardium, develops APD alternans before the epicardium [44]. This differential susceptibility to APD alternans is attributed to significantly reduced endocardial expression of ryanodine release channel and SERCA2 pump compared to the epicardium, suggesting a potentially Cai-based mechanism for the development of spatially heterogeneous APD alternans in the ventricle [40, 44].

The importance of Cai in regulating APD dynamics is not surprising because the membrane voltage and Cai are bidirectionally coupled. This indicates that the APD directly affects the Cai transient amplitude and instabilities of the Cai dynamics can in turn affect the APD [42, 45, 46]. For example, the voltage influences the Cai via the $I_{Ca\text{-}L}$ current which plays a major role in determining both the APD and the amplitude of the Cai transient. The larger the $I_{Ca\text{-}L}$ the longer will be the APD with a larger associated Cai transient amplitude. So if APD alternates between short and long the Cai will passively follow the voltage with small and large ampli-

tude Cai transient, because larger $I_{Ca\text{-}L}$ will cause grater release of Ca from the sarcoplasmic reticulum (SR) while smaller amplitude $I_{Ca\text{-}L}$ will release smaller amount of SR Ca. With this respect, voltage to Cai coupling is positive, i.e., a longer APD produces a larger Cai transient, while shorter APD produces small Cai transient. With respect to Cai influencing the voltage, it is known that the Cai transient amplitude strongly modulates APD through its effects on Ca-sensitive currents during the AP plateau which can be of variable amplitude and thus causing Cai to voltage coupling dynamic scenario to produce either positive or negative coupling. Positive Cai to voltage coupling refers to the mode in which a larger Cai transient produces a longer APD. This occurs when the large Cai transient enhances net inward current during the action potential plateau by potentiating the inward Na–Ca exchange current (forward mode of NCX activation) caused by pumping 3 sodium ions in and one calcium ion out. The generated net inward current under the positive-coupling scenario is greater than the reduction of the $I_{Ca\text{-}L}$ current caused by Ca-induced inactivation of the $I_{Ca\text{-}L}$. On the other hand, negative Cai to voltage coupling could emerge when a larger Cai transient causes a shorter APD, a scenario that emerges when greater reduction in $I_{Ca\text{-}L}$ current occurs due to Cai-mediated inactivation of $I_{Ca\text{-}L}$ over the increased Na–Ca exchange inward current [42, 43, 47]. Other Ca-sensitive currents may also play a role in the strength of Cai to voltage coupling but their influence in affecting the APD are quantitatively less important. These are the Ca-activated nonselective cation current and Ca-activated Cl currents [42, 48].

Causes of dynamic instability of Ca_i^{+2}: Experimental and simulation studies suggest that a steep sarcoplasmic reticulum (SR) load vs. SR Ca release relationship coupled with a slowed rate of uptake of the released Ca back to the SR by the SERCA pump promote Cai dynamic instability (i.e., Cai alternans) which in turn could then promote APD alternans. Diaz et al [49] proposed that Cai alternans arises primarily by a steep dependence of the amount of SR Ca release on the SR Ca load. Using isolated rat ventricular myocytes, these investigators showed that Cai^{2+} alternans is due to changes of the SR Ca^{2+} content [50], with the larger amplitude Cai transients resulting from high SR Cai^{2+} content and the smaller ones from an SR with lower Cai^{2+} content [49]. Interestingly, when after a large transient, the SR Ca^{2+} content was artificially elevated by a brief exposure of the cell to a Na^{+}-free solution, then the alternans was interrupted and the next transient was also large suggesting that changes of SR Cai^{2+}content are sufficient to produce alternans [49]. Simulation studies consistent with isolated myocytes experiments showed the importance of the SR Ca load vs. Ca release relationship. When the slope of the SR Ca content vs. SR Ca release relationship was steep, i.e., >1, Ca_i^{2+} alternans emerged and conversely when the slopes were shallower no Ca_i^{2+} alternans emerged. Interestingly, when we coupled shallower slope (i.e.,<1) of SR load vs. SR release curve with critically slow rates of SR Ca_i^{2+} reuptake, Ca_i^{2+} alternans emerged [51]. These findings indicate that instabilities of Cai dynamics arise independent of AP dynamics both in experimental [52] and human studies during open-heart surgery [53].

Conduction velocity (CV) restitution and the emergence of SDA

CV like APD is also sensitive to the preceding DI, and the CV vs. DI relationship which is called the CV restitution curve. The CV restitution curve is typically flat at long DI but decreases at short DIs because of incomplete recovery from inactivation of the fast Na current (I_{Na}) causing slowing of CV. The slowing of the conduction allows the DI to lengthen slightly at sites away from the pacing site causing the APD to lengthen at the site distal to the pacing site. Important slowing of the conduction at the distal site occurs when the slope of the CV restitution curve is steep so that a small delay in conduction engages longer delays at the distal site causing greater prolongation of the APD as defined by the APD restitution curve. Consequently, at rapid rates of activation when the steep portion of the CV restitution curve becomes engaged then the SDA emerges [42, 43, 54, 55]. During SDA some regions of the tissue alternate in a long-short-long APD pattern, while other regions simultaneously alternate in the opposite short-long-short APD pattern as shown in **Figure 2**. These out-of phase regions are separated by a nodal line, in which no alternans is present [42, 56, 57]. At a nodal line, the spatial gradients in APD are the steepest, predisposing to localized conduction block leading to reentry [18, 20]. Clearly reduced I_{Na}

availability such that occur with drugs [58], or during either acute or chronic ischemia [59, 60], increases the range of DI over which CV varies greatly (steep portion of the curve) promoting spatially discordant alternans and increased risk or reentry formation [61]. In addition to steep CV restitution, Ca_i^{2+} dynamics can also bring about SDA [43]. Discordant alternans can be formed, independently of CV restitution, when cellular Cai transient and APD are electromechanically out of phase, i.e., a large-small-large Ca_i^{2+} transient corresponds to a short-long-short APD [43]. When the Cai to voltage coupling is positive, such that alternans at the single-cell level is electromechanically in phase, then Ca_i^{2+} transient alternans in neighboring cells will synchronize. On the other hand, if the Ca_i^{2+} to voltage coupling is negative such that single-cell alternans is electromechanically out of phase, then Ca_i^{2+} transient alternans desynchronize. In this case the Ca_i^{2+} transient alternans can reverse phase over a length scale of one cell, whereas APD alternans reverses phase over a much longer length scale set by the electrotonic coupling leading to SDA [42, 43]. The importance of sufficiently steep CV-restitution required to initiate discordant alternans is needed only when the Ca_i^{2+} transient and APD are in phase [42, 43]. The transition from a single reentrant or a focal VT to VF in the intact heart occur via the emergence of SDA alternans that lead to wavebreak causing a transition from VT to VF [20, 21, 62].

Ectopic beat, tissue & repolarization heterogeneities, cellular coupling & SDA

Another mechanism by which SDA emerges after a concordant alternans is the occurrence of an ectopic beat. The role of the ectopic beat in the transition from spatially concordant to SDA is demonstrated to occur in one and two dimensional (1D & 2D respectively) simulated cardiac tissue. It is shown that the ectopic beat arising after a short DI creates an asymmetric distribution of DIs so during the next beat the APD will be short at one side of the asymmetry but long at the other [55]. Phase reversal in the sequence of mechano-electrical alternans has also been shown to occur during premature stimulation in isolated cat myocytes [63].

Tissue heterogeneities, i.e., pre-existing APD gradient, may facilitate the emergence of SDA without the need for an ectopic beat as the heterogeneity of the APD breaks the symmetry of DI distribution promoting SDA [42, 54, 64]. Local tissue heterogeneities can also promote wavebreak(s) and subsequent wavefront disorganization in situ hearts promoting reentrant VT/VF [65]. Simulation studies have shown that reducing gap junctional facilitates the emergence of SDA via its influence on CV restitution [61]. Subsequent experimental studies have shown that the restoration of the gap junctional conductance with rotigaptide in ischemic guinea pig hearts, improved conduction and eliminated SDA [66]. Finally, anatomic barriers may also promote SDA. A study by Pastore et al has shown that surgical induction of structural barrier over the ventricle of guinea pig hearts promoted SDA. It was suggested that structural barriers facilitate the development of SDA between cells with different ionic properties by electrotonically uncoupling neighboring regions of myocardium and that such mechanism could explain why arrhythmia-prone patients with structural heart disease exhibit T-wave alternans at lower heart rates [67]. The surviving epicardial border zone of canine infarcts is also characterized with reduced gap junctional connexin43 distribution [68] and an increased propensity of wavebreak and reentrant excitation presumably caused by the increased asymmetry of DI distribution [69].

Alternans vs. diffusive current & wavefront curvature

There is strong evidence that axial current flow through the gap junction between the cells (diffusive current) affects not only the CV but cellular repolarization and the APD restitution in a rate-dependent manner [70-72]. This indicates that in addition to intrinsic ionic current properties the intercellular axial current could also affect the APD and APD restitution [71]. For example it is shown in isolated-perfused guinea pig hearts that when a premature electrical stimulus is applied at short coupling intervals the APD of cells located near <3 mm from the site of the stimulating electrode fail to shorten. This site is presumed to correspond to the site of the earliest repolarization (i.e., the site of the earliest depolarization repolarizes first), thus deviating from the classical APD restitution curve profile [71]. However, when the pacing electrode was placed remote from the identical recording site the APD shortened exponentially with progressive increase in the prematurity of

applied stimuli (i.e., stimuli applied at shorter DIs). It is further shown that stronger currents of stimulation result in even more shallower APD restitution curve in cells located <3mm from the stimulating electrode and an onset of APD alternans at a faster pacing rates [71]. Simulation shows that the departure from the classical restitution profile of cells located near the pacing electrode is attributed to depolarizing axial current present in regions of steep repolarization gradients [71].

Effects of curvature: In addition to the active properties of the cardiac cell membranes and the passive electrical characteristics of the network formed by these cells, the geometry of the excitation wavefronts (curvature) may play an important role in defining the speed of propagation causing slowing of propagation and conduction block [73]. Convex wavefronts (positive curvature) have slower speed than flat wavefronts (zero curvature) and concave wavefronts (negative curvature) have faster speed than flat or convex wavefronts [74]. The APD of cells located on wavefronts with positive curvature have longer APD than cells in the region of negative curvature [74]. Curvature of the wave not only changes the conduction velocity and APD and their restitution properties, but also modulate local stability of the spiral wave, resulting in distinct spiral wave phenotypes, including meandering spirals and spiral breakup [74, 75]. In 3D simulated studies, curvature induced by myocardial fiber rotation causes bending of the scroll wave filament (i.e., the line around which the scroll wave rotates) leading to scroll wave breakup that coverts VT to VF [75].

Alternans and short-term cardiac memory

Short-term cardiac memory τ, is defined as the time needed to change the APD in response to a change in the pacing rate (i.e., APD accommodation). Memory has been shown to limit the reliability of the APD restitution slope criterion in predicting the onset of APD alternans [76], while at the same time greatly affecting the stability of nodal lines and the spatial distribution pattern of SDA in the heart [57]. Simulation studies suggest that APD restitution plots relating the APD to the preceding diastolic interval as well as to the preceding APD (thereby containing some degree of memory) one can observe a stable 1:1 response pattern even when the slope of the APD restitution curve is >1 [76]. In these simulation studies, the degrees of short term cardiac "memory" was represented by changing the duration of the previous AP, with longer APD reflecting larger short-term cardiac memory and shorter APD reflecting smaller short-term memory [76]. By interacting short-term cardiac memory with the CV restitution kinetics, SDA manifests a complex spatial-temporal pattern. For example, a recent optical mapping study in the whole rabbit heart suggests that the presence of short-term cardiac memory, i.e., larger time constant of APD accommodation, tends to destabilize the nodal lines causing them to drift during the onset of SDA. This finding indicates that areas of the heart with larger short-term memory promotes instability of the nodal lines promoting complex spatiotemporal oscillations in the heart [57], a pattern that we shown in *in situ* canine heart to promote wavebreak and VF [65]. The importance of larger short-term memory in causing nodal lines to drift is further emphasized by the observation of stable nodal lines in the regions of the heart that manifest smaller short-term memory implied by the display of steep CV restitution vs. CV alternans relationship [57]. The complex spatiotemporal pattern of APD alternans that emerges in the heart represents a form of bifurcation mechanism characterized by a spatial mode of instability that lead to pattern formation, not unlike the Turing instability described in chemical reactions [77]. In his 1952 ground breaking paper [77] Alan Turing, the underappreciated great genius of the 20th century whose 1952 seminal paper was republished again in 1990 given its great importance [78], used a set of differential equations to describe how chemical instability characterized by reaction of chemical reactants followed by diffusion causes spontaneous patterns to form now known as "Turing patterns" [77, 79]. Turing discovered that in order for spatial patterns to form the reaction-diffusion of the chemical reactants in the medium must manifest short range activation and long range inhibitory properties [77]. It is reasonable to equate cardiac depolarization (activation) to "short range activation" while cardiac repolarization (refractoriness) to "long-range inhibition", thus conceptually providing the necessary "reactants" to form a spatial pattern in the heart ("diffusion medium") [79]. The complex spatial mode of APD distribution and activation intervals (bifurcation) that emerges

during heart rate acceleration observed in experimental studies [57, 65] bear analogy to the dynamic theory of spatial pattern formation formulated by Turing sixty years ago [77].

Hopf-homoclinic bifurcation & EAD-mediated triggered activity

The initiation of VT/VF by the mechanism of EAD-mediated triggered activity observed in experimental studies may also be the cause of TdP and polymorphic VT in man [80-82]. Given the importance of the EADs in the genesis of potentially lethal tachyarrhythmias [14, 20, 21, 25-27] much work was vested to understand the ionic and the dynamic mechanisms of these rapid oscillatory membrane depolarizations that suddenly interrupt the normal repolarization of a regular rhythm to cause VT. Unlike the classical mechanism of "automaticity", triggered activity can not be initiated without a prior action potential. That is, while automaticity can be initiated spontaneously in an otherwise quiescent tissue, for triggering to occur by the EAD mechanism a prior action potential is necessary [83]. Using combined experimental, simulation and nonlinear dynamical analyses, much insight is now gained into the mechanisms of EAD that could pave the way for novel and effective therapeutic approaches against VT/VF that were previously unforeseen [8]. The defining feature of the EAD-mediated triggered activity is that it arises during either phase 2 [84] or phase 3 [85, 86] of the action potential before the membrane potential has fully repolarized to the resting level. This is a dynamical example of self-excited oscillatory behavior which often self-terminates is consistent with the dynamical signature of the dual Hopf-homoclinic bifurcations [13, 14] that is amply described to emerge in nonlinear dynamical systems including diverse biological phenomena such as cell cycle [87], pacemaking in neurons and heart [88], glycolytic oscillations [89], and circadian rhythms [90].

The Hopf bifurcation may remain dynamically stable, in that its repetitive motion in the state space plot becomes represented by repeated closed loop trajectories known as stable limit cycle attractor. The repeating periodic loops will remain on the same closed loop orbit as long as the limit cycle remains stable that is, no change in key parameter(s) of the system develop(s) during the evolution of the limit cycle. EAD-mediated focal triggered activity in the ventricle could cause focal VT as shown in **Figure 3**. Since cardiac cellular homeostasis can not remain stable during very rapid repetitive activity, changes in key parameter(s) of the cell function causes the original attracting orbits of the limit cycle to repel. The repelled orbits of the unstable limit cycle end up on a trajectory with infinite period causing termination of the oscillation. This dynamic transition that terminates the unstable limit cycle after an initial slowing of its period is known as homoclinic bifurcation or saddle point bifurcation. Thus the initiation and termination of EAD-mediated triggered activity can be adequately represented by the dual Hopf-homoclinic bifurcation dynamics [13, 14]. In order to define the ionic basis of the Hopf-homoclinic bifurcation hypothesis of EAD-mediated triggered activity and its termination we used a relatively simple three variable model of simulated ventricular action potential. The three variables were the rate constant of activation and inactivation of the inward L-type Ca current ($I_{Ca\text{-}L}$) and the rate constant of activation of a generic potassium outward current [13]. Using these three variables we reproduced the Hopf-homoclinic bifurcation when the three time constants of the two currents coincided in time and voltage with values that exert a periodic influence on each other. Specifically, the EADs were produced when the activation rate of the outward potassium current was delayed in the Ca window voltage range so to allow reactivation of $I_{Ca\text{-}L}$ to be manifested unhampered [13]. The Ca window voltage range is the range of voltages where the steady-state activation and inactivation curves the $I_{Ca\text{-}L}$ intersect. This means that the within this voltage range (-10 mV to -45 mV) the L-type Ca channel remains always open. Should outward potassium current activation remain delayed within this voltage range then the EADs will emerge. In contrast, should the potassium becomes activated in the Ca window voltage range, then the EADs will be suppressed [13]. The results of this simplified cardiac cell model provides proof-of-concept that a mere kinetic manipulation of the inward and outward current in the Ca window current range critically defines the initiation and or suppression of EADs. In order to gain further insight into the ionic mechanisms of Hopf-homoclinic dynamic scenario we [14] recently used a more realistic cardiac cell model which includes a

detailed Ca_i^{2+} cycling and ionic fluxes [91]. We found that during the EAD-mediated triggered activity (Hopf bifurcation) the intracellular sodium ion concentration (Na_i^+) progressively rises which in turn activates the electrogenic outward Na-K pump current (I_{NaK}). The amplitude of the generated outward current progressively increases during the evolution of the triggered activity eventually becoming large enough to counter the reactivation of $I_{Ca\text{-}L}$ in the Ca window voltage range thus terminating the triggered activity after an initial slowing. This dynamic profile is consistent with the homoclinic bifurcation [14]. The key role played by the rise in Na_i^+ in the termination of the triggered activity is further emphasized by clamping its rise and demonstrating the persistence of the triggered activity in our simulation studies [14]. These studies point that the ionic counterpart of the Hopf bifurcation is the repetitive reactivation of I_{CaL} with critically delayed activation of the outward current and that the homoclinic bifurcation emerges when the rise in Na_i^+ promotes outward current by activating the electrogenic Na^+-K^+ pump thus preventing EAD formation and subsequent triggering. An important practical usefulness of the dynamic analyses of EAD-mediated triggered activity is the ability of the Hopf-homoclinic bifurcation scenario to explain why EADs become suppressed with further reduction in repolarization reserve [13, 14]. We investigated in neonatal rat ventricular monolayers the role of further reducing the repolarization reserve on Bay K8644 and isoproterenol-induced EADs and triggered activity. By using two different methods of repolarization reserve reduction (block of transient outward current, Ito, and prevention of the inactivation of $I_{Ca\text{-}L}$ with mutant calmodulin that does not bind to Ca ions) the EADs were suppressed by these two interventions despite excessive prolongation of the APD [14]. A practical take of these findings is that it explains the apparent paradox of why some type of prolongation of the QT interval in patients with the LQT syndrome do not develop Torsade de pointes while others do [92]. AP prolongation per se is much less prone to cause EADs if the plateau voltage remains above the voltage range of I_{CaL} reactivation, i.e., Ca window voltage. If the voltage during the AP plateau remains prolonged but above the voltage range of Ca window current then no EADs emerge despite excessive prolongation of the APD [93]. The Hopf-homoclinic bifurcation can also predict a third form of termination of oscillation, namely the mechanism of failed repolarization [94, 95]. Our simulation shows that non-repolarizing action potentials (bistable regime) [14, 15] occur by simply altering the conductance of the $I_{Ca\text{-}L}$ and the time constant of the potassium current activation. With a critical rise in the $I_{Ca\text{-}L}$ conductance a stable and persistent action potential plateau (failed repolarization) emerges that becomes maintained by the Ca window current independent of the activation time constant of the potassium outward current [14]. However, with time a further eventual increase in the outward current terminates the state of failed repolarization by bringing the membrane potential back to the resting state [13, 14].

The predictions made by the Hopf-homoclinic bifurcation can also help develop therapeutic strategies to prevent the emergence of EADs and triggered activity. The strategy is based on altering the kinetics of the Ca window current by either decreasing its size or flattening the steepness of the steady-state activation and inactivation curves of the $I_{Ca\text{-}L}$ without interfering with Ca_i^{2+} transient and excitation-contraction coupling. Phase 2 EADs are initiated between -40 and 0 mV corresponding to the range of membrane voltages where the steady-state activation and inactivation curves of $I_{Ca\text{-}L}$ overlap (i.e., 'Ca window current') [84, 96]. As the AP repolarizes into this voltage 'window' range, a fraction of the $I_{Ca\text{-}L}$ that are not inactivated become available for reactivation to generate the upstroke of the EAD. By adopting the recently introduced technique of hybrid biological–computational approach, i.e., the dynamic-clamp technique [97] we replaced the native $I_{Ca\text{-}L}$ of the myocyte with a computed virtual $I_{Ca\text{-}L}$ with programmable properties [8]. We found, as expected by the Hopf bifurcation theory [13], that the formation of the EAD is highly sensitive to the kinetics of activation and inactivation of the $I_{Ca\text{-}L}$ in the window region, such that subtle shifts in the voltage dependence of steady-state $I_{Ca\text{-}L}$ activation or inactivation can abolish EADs without affecting the amplitude or kinetics of the intracellular Ca^{2+} transient (i.e., preserved normal excitation-contraction coupling) [8]. These findings are encouraging in that they demonstrate 'proof-of-concept' of drug therapy against EADs can be designed by manipulating the kinetics of activation and inactivation of the

$I_{Ca\text{-}L}$ without affecting myocardial contractility. Interestingly, whereas pharmacological agents may have off-target effects in both cardiac and non-cardiac tissue. A specific way to target $I_{Ca\text{-}L}$ could be to take advantage of the modulatory accessory (beta) subunits of the L-type Ca channels [98] to bring about the desired kinetic properties of the $I_{Ca\text{-}L}$ to prevent EADs [8].

Clinical impact

In the 1990s, human clinical trials conclusively established the link between cardiac alternans, in the form of electrocardiographic T wave alternans, and the emergence of reentrant VT/VF in man [33, 34]. Similarly, the evidence linking EAD to triggered activity and Torsade de Pointes in humans is also mounting and increasingly appreciated [14]. Since both of these mechanisms increase the risk of sudden cardiac death in man and since the dynamic mechanisms of both of these two types of arrhythmias are compatible with the period doubling and Hopf-homoclinic bifurcation theories respectively, it is hoped that the bifurcation theory may provide novel insight and therapeutic potentials to control sudden cardiac death caused by VF in man. The example of manipulating the kinetics of activation and inactivation of $I_{Ca\text{-}L}$ described here is a promising novel and effective therapeutic strategy against VF without compromising the normal excitation-contraction coupling process [8].

Acknowledgements

This study was supported in part by NIH Grant P01 HL78931.

Address correspondence to: Dr. Hrayr S Karagueuzian, Translational Arrhythmia Research Section, Cardiovascular Research Laboratory, David Geffen School of Medicine at UCLA, 675 Charles E. Young Dr. South MRL 1630. Mail Code: 176022; Phone: 310-825-9360; Fax: 310-206-5777; E-mail: HKaragueuzian@mednet.ucla.edu

References

[1] Winfree AT. Electrical instability in cardiac muscle: phase singularities and rotors. J Theor Biol 1989 Jun 8; 138: 353-405.

[2] Glass LM. From Clock to Chaos: The Rhythm of Life. Princeton University 1987.

[3] Krogh-Madsen T and Christini DJ. Nonlinear dynamics in cardiology. Annu Rev Biomed Eng 2012; 14: 179-203.

[4] Poincaré H. L'Équilibre d'une masse fluide animée d'un mouvement de rotation. Acta Mathematica 1885; t7: 259-380.

[5] Guevara MR, Glass L and Shrier A. Phase locking, period-doubling bifurcations, and irregular dynamics in periodically stimulated cardiac cells. Science 1981; 214: 1350-1353.

[6] Glass L and Zeng WZ. Complex bifurcations and chaos in simple theoretical models of cardiac oscillations. Ann N Y Acad Sci 1990; 591: 316-27.

[7] Garfinkel A, Spano ML, Ditto WL and Weiss JN. Controlling cardiac chaos. Science 1992; 257: 1230-1235.

[8] Madhvani RV, Xie Y, Pantazis A, Garfinkel A, Qu Z, Weiss JN and Olcese R. Shaping a new Ca(2)(+) conductance to suppress early afterdepolarizations in cardiac myocytes. J Physiol 2011; 589: 6081-6092.

[9] Chialvo DR, Michaels DC and Jalife J. Supernormal excitability as a mechanism of chaotic dynamics of activation in cardiac purkinje fibers. Circ Res 1990; 66: 525-545.

[10] Chialvo DR, Gilmour RF Jr and Jalife J. Low dimensional chaos in cardiac tissue. Nature 1990; 343: 653-657.

[11] Gilmour RF Jr, Watanabe M and Chialvo DR. Low dimensional dynamics in cardiac tissues. Experiments and theory. Chaos in biology and Medicine 1993; 2036: 1-9.

[12] Karagueuzian HS, Khan SS, Hong K, Kobayashi Y, Denton T, Mandel WJ and Diamond GA. Action potential alternans and irregular dynamics in quinidine-intoxicated ventricular muscle cells. Implications for ventricular proarrhythmia. Circulation 1993; 87: 1661-1672.

[13] Tran DX, Sato D, Yochelis A, Weiss JN, Garfinkel A and Qu Z. Bifurcation and chaos in a model of cardiac early afterdepolarizations. Phys Rev Lett 2009; 102: 258103.

[14] Chang MG, Chang CY, de Lange E, Xu L, O'Rourke B, Karagueuzian HS, Tung L, Marban E, Garfinkel A, Weiss JN, Qu Z and Abraham MR. Dynamics of early afterdepolarization-mediated triggered activity in cardiac monolayers. Biophys J 2012; 102: 2706-2714.

[15] Chang MG, Sato D, de Lange E, Lee JH, Karagueuzian HS, Garfinkel A, Weiss JN and Qu Z. Bi-stable wave propagation and early afterdepolarization-mediated cardiac arrhythmias. Heart Rhythm 2012; 9: 115-122.

[16] Konta T, Ikeda K, Yamaki M, Nakamura K, Honma K, Kubota I and Yasui S. Significance of discordant ST alternans in ventricular fibrillation. Circulation 1990; 82: 2185-2189.

[17] Pastore JM, Girouard SD and Rosenbaum DS. Mechanism of initiation of ventricular fibrillation during T wave alternans. Pacing and Cardiac Electrophysiology 1997; 20: 1196-1196.

[18] Pastore JM, Girouard SD, Laurita KR, Akar FG and Rosenbaum DS. Mechanism linking T-wave alternans to the genesis of cardiac fibrillation. Circulation 1999; 99: 1385-1394.

[19] Fox JJ, Riccio ML, Hua F, Bodenschatz E and Gilmour RF Jr. Spatiotemporal transition to conduction block in canine ventricle. Circ Res 2002; 90: 289-296.

[20] Morita N, Sovari AA, Xie Y, Fishbein MC, Mandel WJ, Garfinkel A, Lin SF, Chen PS, Xie LH, Chen F, Qu Z, Weiss JN and Karagueuzian HS. Increased Susceptibility of Aged Hearts to Ventricular Fibrillation During Oxidative Stress. Am J Physiol Heart Circ Physiol 2009; 297: H1594-H1605.

[21] Morita N, Lee JH, Bapat A, Fishbein MC, Mandel WJ, Chen PS, Weiss JN and Karagueuzian HS. Glycolytic Inhibition Causes Spontaneous Ventricular Fibrillation in Aged Hearts. Am J Physiol Heart Circ Physiol 2011; 301: H180-H191.

[22] Avitall B, Naimi S, Brilla AH and Levine HJ. A computerized system for measuring dispersion of repolarization in the intact heart. J Appl Physiol 1974; 37: 456-458.

[23] Amlie JP, Kuo CS, Munakata K, Reddy PS and Surawicz B. Effect of uniformly prolonged, and increased basic dispersion of repolarization on premature dispersion on ventricular surface in dogs: role of action potential duration and activation time differences. Eur Heart J 1985 Nov; 6: 15-30.

[24] Kuo CS, Munakata K, Reddy CP and Surawicz B. Characteristics and possible mechanism of ventricular arrhythmia dependent on the dispersion of action potential durations. Circulation 1983; 67: 1356-1367.

[25] Asano Y, Davidenko JM, Baxter WT, Gray RA and Jalife J. Optical mapping of drug-induced polymorphic arrhythmias and torsade de pointes in the isolated rabbit heart. J Am Coll Cardiol 1997; 29: 831-842.

[26] Choi BR, Burton F and Salama G. Cytosolic Ca^{2+} triggers early afterdepolarizations and Torsade de Pointes in rabbit hearts with type 2 long QT syndrome. J Physiol 2002 Sep 1; 543: 615-31.

[27] Sato D, Xie LH, Sovari AA, Tran DX, Morita N, Xie F, Karagueuzian H, Garfinkel A, Weiss JN and Qu Z. Synchronization of chaotic early afterdepolarizations in the genesis of cardiac arrhythmias. Proc Natl Acad Sci U S A 2009; 106: 2983-2988.

[28] Rubart M and Zipes DP. Mechanisms of sudden cardiac death. J Clin Invest 2005; 115: 2305-2315.

[29] Ono N, Hayashi H, Kawase A, Lin SF, Li H, Weiss JN, Chen PS and Karagueuzian H. Spontaneous atrial fibrillation initiated by triggered activity near the pulmonary veins in aged rats subjected to glycolytic inhibition. Am J Physiol Heart Circ Physiol 2007; 292: 639-648.

[30] Blatter LA, Kockskamper J, Sheehan KA, Zima AV, Huser J and Lipsius SL. Local calcium gradients during excitation-contraction coupling and alternans in atrial myocytes. J Physiol 2003; 546: 19-31.

[31] Garfinkel A, Kim YH, Voroshilovsky O, Qu Z, Kil JR, Lee MH, Karagueuzian HS, Weiss JN and Chen PS. Preventing ventricular fibrillation by flattening cardiac restitution. Proc Natl Acad Sci U S A 2000; 97: 6061-6066.

[32] Lewis T. Notes upon alternation of the heart. Quart J Med 1910; 4: 141-144.

[33] Rosenbaum DS, Jackson LE, Smith JM, Garan H, Ruskin JN and Cohen RJ. Electrical alternans and vulnerability to ventricular arrhythmias. N Engl J Med 1994; 330: 235-241.

[34] Gehi AK, Stein RH, Metz LD and Gomes JA. Microvolt T-wave alternans for the risk stratification of ventricular tachyarrhythmic events: a meta-analysis. J Am Coll Cardiol 2005; 46: 75-82.

[35] Nolasco JB and Dahlen RW. A graphic method for the study of alternation in cardiac action potentials. J Appl Physiol 1968; 25: 191-196.

[36] Franz MR, Schaefer J, Schottler M, Seed WA and Noble MI. Electrical and mechanical restitution of the human heart at different rates of stimulation. Circ Res 1983 Dec; 53: 815-22.

[37] Guevara MR, Shrier A and Glass L. Electrical alternans and period-doubling bifurcations. Computers in Cardiology 1984; 1: 167-170.

[38] Chialvo DR and Jalife J. Non-linear dynamics of cardiac excitation and impulse propagation. Nature 1987; 330: 749-752.

[39] Garfinkel A, Chen PS, Walter DO, Karagueuzian HS, Kogan B, Evans SJ, Karpoukhin M, Hwang C, Uchida T, Gotoh M, Nwasokwa O, Sager P and Weiss JN. Quasiperiodicity and chaos in cardiac fibrillation. J Clin Invest 1997 Jan 15; 99: 305-14.

[40] Pruvot EJ, Katra RP, Rosenbaum DS and Laurita KR. Role of calcium cycling versus restitution in the mechanism of repolarization alternans. Circ Res 2004 Apr 30; 94: 1083-90.

[41] Goldhaber JI, Xie LH, Duong T, Motter C, Khuu K and Weiss JN. Action potential duration restitution and alternans in rabbit ventricular myocytes: the key role of intracellular calcium cycling. Circ Res 2005; 96: 459-466.

[42] Weiss JN, Karma A, Shiferaw Y, Chen PS, Garfinkel A and Qu Z. From pulsus to pulseless: the saga of cardiac alternans. Circ Res 2006 May 26; 98: 1244-53.

[43] Sato D, Shiferaw Y, Garfinkel A, Weiss JN, Qu Z and Karma A. Spatially discordant alternans in

cardiac tissue: role of calcium cycling. Circ Res 2006; 99: 520-527.

[44] Wan X, Laurita KR, Pruvot EJ and Rosenbaum DS. Molecular correlates of repolarization alternans in cardiac myocytes. J Mol Cell Cardiol 2005; 39: 419-428.

[45] Eisner DA, Choi HS, Diaz ME, O'Neill SC and Trafford AW. Integrative analysis of calcium cycling in cardiac muscle. Circ Res 2000; 87: 1087-1094.

[46] Eisner DA, Diaz ME, Li Y, O'Neill SC and Trafford AW. Stability and instability of regulation of intracellular calcium. Exp Physiol 2005; 90: 3-12.

[47] Sato D, Shiferaw Y, Garfinkel A, Weiss JN, Qu Z and Karma A. Spatially discordant alternans in cardiac tissue: role of calcium cycling. Circ Res 2006; 99: 520-527.

[48] Aggarwal R, Pu J and Boyden PA. Ca(2+)-dependent outward currents in myocytes from epicardial border zone of 5-day infarcted canine heart. Am J Physiol 1997 Sep; 273: H1386-94.

[49] Diaz ME, O'Neill SC and Eisner DA. Sarcoplasmic reticulum calcium content fluctuation is the key to cardiac alternans. Circ Res 2004; 94: 650-656.

[50] Bassani JW, Yuan W and Bers DM. Fractional SR Ca release is regulated by trigger Ca and SR Ca content in cardiac myocytes. Am J Physiol 1995 May; 268: C1313-9.

[51] Shiferaw Y, Watanabe MA, Garfinkel A, Weiss JN and Karma A. Model of intracellular calcium cycling in ventricular myocytes. Biophys J 2003; 85: 3666-3686.

[52] Qian YW, Clusin WT, Lin SF, Han J and Sung RJ. Spatial heterogeneity of calcium transient alternans during the early phase of myocardial ischemia in the blood-perfused rabbit heart. Circulation 2001; 104: 2082-2087.

[53] Taggart P, Sutton PM, Boyett MR, Lab M and Swanton H. Human ventricular action potential duration during short and long cycles. Rapid modulation by ischemia. Circulation 1996; 94: 2526-2534.

[54] Qu Z, Garfinkel A, Chen PS and Weiss JN. Mechanisms of discordant alternans and induction of reentry in simulated cardiac tissue. Circulation 2000; 102: 1664-1670.

[55] Watanabe MA, Fenton FH, Evans SJ, Hastings HM and Karma A. Mechanisms for discordant alternans. J Cardiovasc Electrophysiol 2001 Feb; 12: 196-206.

[56] Hayashi H, Shiferaw Y, Sato D, Nihei M, Lin SF, Chen PS, Garfinkel A, Weiss JN and Qu Z. Dynamic origin of spatially discordant alternans in cardiac tissue. Biophys J 2007; 92: 448-460.

[57] Mironov S, Jalife J and Tolkacheva EG. Role of conduction velocity restitution and short-term memory in the development of action potential duration alternans in isolated rabbit hearts. Circulation 2008; 118: 17-25.

[58] Pu J, Balser JR and Boyden PA. Lidocaine action on Na+ currents in ventricular myocytes from the epicardial border zone of the infarcted heart. Circ Res 1998 Aug 24; 83: 431-40.

[59] Pu J and Boyden PA. Alterations of Na+ currents in myocytes from epicardial border zone of the infarcted heart. A possible ionic mechanism for reduced excitability and postrepolarization refractoriness. Circ Res 1997; 81: 110-119.

[60] Joyner RW, Ramza BM, Osaka T and Tan RC. Cellular mechanisms of delayed recovery of excitability in ventricular tissue. Am J Physiol 1991 Jan; 260: H225-33.

[61] Qu Z, Karagueuzian HS, Garfinkel A and Weiss JN. Effects of Na+ Channel and Cell Coupling Abnormalities on Vulnerability to Reentry: A Simulation Study. Am J Physiol Heart Circ Physiol 2004; 286: 1310-1321.

[62] Morita N, Lee JH, Xie Y, Sovari A, Qu Z, Weiss JN and Karagueuzian HS. Suppression of re-entrant and multifocal ventricular fibrillation by the late sodium current blocker ranolazine. J Am Coll Cardiol 2011; 57: 366-375.

[63] Rubenstein DS and Lipsius SL. Premature beats elicit a phase reversal of mechanoelectrical alternans in cat ventricular myocytes. A possible mechanism for reentrant arrhythmias. Circulation 1995; 91: 201-214.

[64] Pastore JM, Laurita KR and Rosenbaum DS. Importance of spatiotemporal heterogeneity of cellular restitution in mechanism of arrhythmogenic discordant alternans. Heart Rhythm 2006; 3: 711-719.

[65] Cao JM, Qu Z, Kim YH, Wu TJ, Garfinkel A, Weiss JN, Karagueuzian HS and Chen PS. Spatiotemporal heterogeneity in the induction of ventricular fibrillation by rapid pacing: importance of cardiac restitution properties. Circ Res 1999; 84: 1318-1331.

[66] Kjolbye AL, Dikshteyn M, Eloff BC, Deschenes I and Rosenbaum DS. Maintenance of intercellular coupling by the antiarrhythmic peptide rotigaptide suppresses arrhythmogenic discordant alternans. Am J Physiol Heart Circ Physiol 2008; 294: H41-49.

[67] Pastore JM and Rosenbaum DS. Role of structural barriers in the mechanism of alternans-induced reentry. Circ Res 2000; 87: 1157-1163.

[68] Peters NS, Coromilas J, Severs NJ and Wit AL. Disturbed connexin43 gap junction distribution correlates with the location of reentrant circuits in the epicardial border zone of healing

canine infarcts that cause ventricular tachycardia. Circulation 1997; 95: 988-996.
[69] Ohara T, Ohara K, Cao JM, Lee MH, Fishbein MC, Mandel WJ, Chen PS and Karagueuzian HS. Increased wavebreak during ventricular fibrillation in the epicardial border zone of hearts with healed myocardial infarction. Circulation 2001; 103: 1465-1472.
[70] Tan RC and Joyner RW. Electrotonic influences on action potentials from isolated ventricular cells. Circ Res 1990; 67: 1071-1081.
[71] Laurita KR, Girouard SD, Rudy Y and Rosenbaum DS. Role of passive electrical properties during action potential restitution in intact heart. Am J Physiol 1997; 273: H1205-H1214.
[72] Qu Z. Dynamical effects of diffusive cell coupling on cardiac excitation and propagation: a simulation study. Am J Physiol Heart Circ Physiol 2004; 287: H2803-2812.
[73] Fast VG and Kleber AG. Role of wavefront curvature in propagation of cardiac impulse. Cardiovasc Res 1997 Feb; 33: 258-71.
[74] Qu Z, Xie F, Garfinkel A and Weiss JN. Origins of spiral wave meander and breakup in a two-dimensional cardiac tissue model. Ann Biomed Eng 2000; 28: 755-771.
[75] Qu Z, Kil J, Xie F, Garfinkel A and Weiss JN. Scroll wave dynamics in a three-dimensional cardiac tissue model: roles of restitution, thickness, and fiber rotation. Biophys J 2000 Jun; 78: 2761-75.
[76] Tolkacheva EG, Schaeffer DG, Gauthier DJ and Krassowska W. Condition for alternans and stability of the 1:1 response pattern in a "memory" model of paced cardiac dynamics. Phys Rev E Stat Nonlin Soft Matter Phys 2003; 67: 031904.
[77] Turing A. The chemical basis of morphogenesis. Philos Trans R Soc 1952; 237: 37-72.
[78] Turing AM. The chemical basis of morphogenesis. Bull Math Biol 1990; 52: 153-197; discussion 119-152.
[79] Weiss JN, Qu Z and Garfinkel A. Understanding biological complexity: lessons from the past. Faseb J 2003; 17: 1-6.
[80] Moreno JD and Clancy CE. Pathophysiology of the cardiac late Na current and its potential as a drug target. J Mol Cell Cardiol 2012; 52: 608-619.
[81] Ruan Y, Liu N and Priori SG. Sodium channel mutations and arrhythmias. Nat Rev Cardiol 2009; 6: 337-348.
[82] Clancy CE and Kass RS. Inherited and acquired vulnerability to ventricular arrhythmias: cardiac Na+ and K+ channels. Physiol Rev 2005; 85: 33-47.
[83] Cranefield PF. Action potentials, afterpotentials, and arrhythmias. Circ Res 1977; 41: 415-423.
[84] January CT and Riddle JM. Early afterdepolarizations: mechanism of induction and block. A role for L-type Ca^{2+} current. Circ Res 1989; 64: 977-990.
[85] Burashnikov A and Antzelevitch C. Reinduction of atrial fibrillation immediately after termination of the arrhythmia is mediated by late phase 3 early afterdepolarization-induced triggered activity. Circulation 2003; 107: 2355-2360.
[86] Maruyama M, Lin SF, Xie Y, Chua SK, Joung B, Han S, Shinohara T, Shen MJ, Qu Z, Weiss JN and Chen PS. Genesis of Phase-3 Early Afterdepolarizations and Triggered Activity in Acquired Long QT Syndrome. Circ Arrhythm Electrophysiol 2011 Feb; 4: 103-11.
[87] Qu Z, MacLellan WR and Weiss JN. Dynamics of the cell cycle: checkpoints, sizers, and timers. Biophys J 2003; 85: 3600-3611.
[88] Guevara MR and Jongsma HJ. Three ways of abolishing automaticity in sinoatrial node: ionic modeling and nonlinear dynamics. Am J Physiol 1992; 262: H1268-1286.
[89] Goldbeter A and Lefever R. Dissipative structures for an allosteric model. Application to glycolytic oscillations. Biophys J 1972; 12: 1302-1315.
[90] Goldbeter A. A model for circadian oscillations in the Drosophila period protein (PER). Proc Biol Sci 1995; 261: 319-324.
[91] Mahajan A, Sato D, Shiferaw Y, Baher A, Xie LH, Peralta R, Olcese R, Garfinkel A, Qu Z and Weiss JN. Modifying L-type calcium current kinetics: consequences for cardiac excitation and arrhythmia dynamics. Biophys J 2008; 94: 411-423.
[92] Hondeghem LM. QT prolongation is an unreliable predictor of ventricular arrhythmia. Heart Rhythm 2008; 5: 1210-1212.
[93] Weiss JN, Garfinkel A, Karagueuzian HS, Chen PS and Qu Z. Early afterdepolarizations and cardiac arrhythmias. Heart Rhythm 2010; 7: 1891-1899.
[94] Bapat A, Nguyen TP, Lee JH, Sovari AA, Fishbein MC, Weiss JN and Karagueuzian HS. Enhanced Sensitivity of Aged Fibrotic Hearts to Angiotensin II- & Hypokalemia-Induced Early Afterdepolarizations-Mediated Ventricular Arrhythmias. Am J Physiol Heart Circ Physiol 2012; 302: H2331-H2340.
[95] Nguyen TP, Xie Y, Garfinkel A, Qu Z and Weiss JN. Arrhythmogenic Consequences of Myofibroblast-Myocyte Coupling. Cardiovasc Res 2012; 93: 242-251.
[96] Antoons G, Volders PG, Stankovicova T, Bito V, Stengl M, Vos MA and Sipido KR. Window Ca^{2+} current and its modulation by Ca^{2+} release in hypertrophied cardiac myocytes from dogs

with chronic atrioventricular block. J Physiol 2007 Feb 15; 579: 147-60.
[97] Dorval AD, Christini DJ and White JA. Real-time linux dynamic clamp: a fast and flexible way to construct virtual ion channels in living cells. Ann Biomed Eng 2001; 29: 897-907.
[98] Dolphin AC. Calcium channel diversity: multiple roles of calcium channel subunits. Curr Opin Neurobiol 2009; 19: 237-244.
[99] Weiss JN, Garfinkel A, Karagueuzian HS, Qu Z and Chen PS. Chaos and the transition to ventricular fibrillation: A new approach to antiarrhythmic drug evaluation. Circulation 1999; 99: 2819-2826.